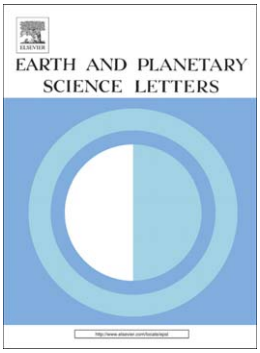

Strength of the lithosphere and strain localisation in the Baikal rift

Carole Petit, Evguene Burov, Christel Tiberi

PII: S0012-821X(08)00165-9
DOI: doi: 10.1016/j.epsl.2008.03.012
Reference: EPSL 9198

To appear in: *Earth and Planetary Science Letters*

Received date: 29 May 2007
Revised date: 28 February 2008
Accepted date: 3 March 2008

Please cite this article as: Carole Petit, Evguene Burov, Christel Tiberi, Strength of the lithosphere and strain localisation in the Baikal rift, *Earth and Planetary Science Letters* (2008), doi: 10.1016/j.epsl.2008.03.012

Strength of the lithosphere and strain localisation in the Baikal rift

Submitted to

Earth and Planetary Science Letters

By

Carole PETIT*, Evguene BUROV and Christel TIBERI

REVISED VERSION – Feb 28th 2008

Laboratoire de Tectonique, CNRS-UPMC, Tour 46-00 E2, Boite 129, 4 Place Jussieu, 75252 PARIS CEDEX 05, France

*Corresponding author
carole.petit@lgs.jussieu.fr

Abstract

We use previously published estimates of Moho and lithosphere-asthenosphere boundary (LAB) depths combined with a 3D thermal model to infer variations of the effective elastic thickness (EET) of the lithosphere in the Baikal rift zone. The predicted continuous EET map is validated using EET values from previous forward flexural models across separate profiles. This map presents a present-day snapshot of the lithosphere mechanical behaviour. It suggests that the cratonic keel bounding the NW part of the rift is characterized by a strong lithosphere where the crust and mantle are mechanically coupled, whereas the more recent (Palaeo-Mesozoic) fold zone located SE of the rift is significantly weaker. Predicted spatial EET variations correlate well with the spatial distribution of earthquakes: where EET abruptly drops from high (~ 50km) to low (~25 km) values, epicentre distribution also changes from very localised to diffuse, suggesting that the degree of crust-mantle coupling responsible for EET drops also controls strain localisation. Finally, we suggest that even though the current thermal state of the lithosphere does not favour partial melting near the LAB depth, the latter could have been promoted in case of moderately hotter lithosphere (+120°C compared to the temperature at the current base). This could be the case during the earlier volcanic period, which spanned from the Oligocene to the Pleistocene.

Introduction

The lithosphere is defined as the outermost, rigid envelope of the earth, comprising the crust and the uppermost mantle. Yet, there is a strong debate concerning the true rigidity of the continental uppermost mantle over geological timescales, which questions its belonging to the lithosphere in its original sense. Indeed, earthquake depth distribution and spectral analyses of gravity data in the continental domain led some authors to conclude that most of the lithosphere rigidity lies within the crust – including its lower part, and that the uppermost mantle has no significant strength [e.g., Emmerson et al., 2006; Maggi et al., 2000]. On the other side, most numerical models of lithosphere deformation successfully reproduce geodynamic processes using a rigid uppermost mantle [e.g., Huismans and Beaumont, 2002; Huismans et al., 2001; Lavier and Manatschal, 2006; Burov and Poliakov, 2001]. Finally, recent seismic studies appear to provide new evidence for the presence of very deep mantle seismicity, at least below actively deforming cratons, which supports the idea of strong mantle [e.g., Monsalve et al., 2006; De la Torre et al., 2007]. According to the "strong mantle" school, the degree of crust-mantle coupling plays a dominant role in the strain localisation because it reflects the competition between localising (i.e., elastic-brittle) and delocalising

diffuse (i.e. elastic-ductile) strain behaviours [e.g., Hopper and Buck, 1998]. For example, in the classical "wide rift" vs. "narrow rift" distinction made by Buck [1991] the rheological layering of the lithosphere exerts a first-order control on the rift geometry: "wide" or "diffuse" rifts are associated with a weak lithosphere whereas "narrow" or "discrete" rifts are zones of well-localised deformation in a relatively strong lithosphere. The crust and mantle parts of the lithosphere can be mechanically coupled provided that the temperature at the Moho is low enough and the lower crust rheology is strong enough to prevent the development of a thick, low-strength ductile lower crust. In some cases, the degree of crust-mantle coupling can be directly assessed from geological or geophysical data like earthquake depths and focal mechanisms [e.g., Mouthereau and Petit, 2003; Stich et al., 2005], GPS or SKS splitting data [e.g., Flesch et al., 2005] or magneto-telluric sounding [e.g. Park et al., 1992]. It can be also assessed indirectly from "decoding" the effective elastic thickness (EET) of the lithosphere. According to the "weak mantle" hypothesis, the effective elastic thickness of continental lithosphere is close to, or lower than the crustal seismogenic thickness, so that crust/mantle coupling does not occur, because the strong mantle does not exist. On the other hand, the "strong mantle" hypothesis predicts high EET values (50-60 km) when the crust and mantle elastic cores are mechanically coupled and an abrupt reduction of EET to values lower than 30 km if they are decoupled [e.g. Burov and Diament, 1995; Watts and Burov, 2003; Burov and Watts, 2006]. Given the effect of crust mantle coupling both on strain localisation and on EET variations, an argument to the "strong mantle" hypothesis should be found in a good spatial correlation between rapid changes from diffuse to localised strain and sharp EET jumps in the case of uncoupled/coupled behaviour transition.

In this paper, we use previously published estimates of Moho, EET and lithosphere asthenosphere boundary (LAB) depths in the Baikal rift [Petit and Déverchère, 2006] to constrain the present-day thermal state and predict the spatial distribution of the effective elastic thickness of the lithosphere, assuming crust and mantle rheologies commonly used in thermo-mechanical numerical models of lithospheric deformation. Then, following the approach developed in [Burov and Diament, 1995, 1996; Burov and Watts, 2006; Watts and Burov, 2003], we validate the predicted EET and, consequently, the assumed rheological parameters using the previous EET estimates obtained from robust forward flexural models. Finally, we compare the results with the spatial distribution of the earthquakes in order to determine how the present-day strength heterogeneities correlate with strain localisation.

The Baikal rift: general setting

The Baikal Rift System is located in northeast Asia, north of the India-Asia collision zone (Fig. 1). It extends over ~1500 km in a ~SW-NE direction and is made of a dozen of small-scale sedimentary basins [Logatchev and Florensov, 1978]. The narrow (60 km) Lake Baikal occupies the central and deepest (up to 9 km including water and sediments infill) part of the rift, and the other basins are emerged. Schematically, the lithosphere of the BRS is composed of two adjacent domains of different ages and structures: 1) the Siberian craton, to the NW, which basement is Archaean and is overlain by a thick Proterozoic to Mesozoic sedimentary cover. 2) the Sayan-Baikal fold belt to the east and southeast, which is made of micro-continents accreted against the craton during the Palaeozoic and Mesozoic (Fig. 1). Rifting started ca. 30 Ma ago in the central part of the rift, but most basins started to develop in the late Miocene [e.g., Petit and Déverchère, 2006 and references therein]. Earthquake epicentres and active faults show that the southern half of the rift localises on the cratonic suture, while the northern half develops within the fold belt and is made of discontinuous en-échelon basins. The main episode of volcanic activity started in the Miocene, although some volcanic emissions occurred as early as 40 Ma ago in the SW part of the rift [Rasskasov et al., 2002]. Miocene to quaternary volcanics outcrop in the SW of the rift in the Hamar-Daban area south of Lake Baikal, east of Lake Baikal in the Vitim region and at the extreme NE of the rift, in the Udokan area (Fig. 1). Most volcanic centers are located off-axis. Eruptions ceased ~600 ka ago, and none of these volcanic centres is still active today.

The geometry of the Moho and LAB have been calculated by Petit and Déverchère [2006] using band-filtering and downward continuation of the Bouguer gravity data, considering that these interfaces are located at different mean depths and thus produce different characteristic wavelengths in the Bouguer gravity signal. The Bouguer anomaly grid comes from gravity survey with original data spacing of about 1' and includes terrain corrections (in a range of 200 km around each data station). This data set was originally produced by Russian Geodetic Service and is available from GETECH (www.getech.com). The density constrasts used are 550 kg/m^3 and 40 kg/m^3 for the Moho and LAB interfaces, respectively. In their parametric study, Petit and Déverchère, [2006] have tested different density contrasts for the Moho (450, 550 and 650 kg/m^3) and LAB (-20, -30 and -40 kg/m^3) to find that the best fit with the observed gravity is achieved for these above referenced values. These values were chosen also because they provide prediction for Moho and LAB depths that are in a good agreement with the previously published data such as deep seismic soundings, tomography models or xenolith data [e.g., ; Gao et al., 2004; Ionov, 2002; Pavlenkova et al., 2002; Suvorov et al.,

2002; Tiberi et al., 2003]. Lateral density contrasts have been neglected because this study was aimed at determining the large-scale lithospheric structure, given the selected gravity wavelengths. However, density contrasts can be present at smaller scale, especially in the crust due to its complicated geological history. The inferred Moho depth ranges between 34 km in the central part of Lake Baikal and more than 48 km in the northern and southern parts of the rift (Fig. 2). The mean crustal thickness in the Siberian craton is 43 km. The lithosphere-asthenosphere boundary is shallowest beneath the Hamar-Daban and Vitim areas (~70 km), yet no significant lithospheric thinning is found at the rift axis. Instead, the lithosphere progressively thickens towards the NW, reaching more than 140 km beneath the core of the Siberian craton (Fig. 2). The depth of the LAB in the Baikal rift is still a matter of debate, as some authors found that it can reach the base of the crust in some places beneath the rift [e.g., Gao et al., 2003], whereas we use a model in which it is never shallower than 70 km. An asthenospheric uplift to depths of 40-50 km beneath the rift is advocated by Gao et al. [2003] for explaining teleseismic traveltime residuals, but the joint inversion of traveltime residuals and gravity data rather place it at greater depths [70 km, Tiberi et al., 2003], which is more consistent with xenolith data [Ionov, 2002]. In addition, a wide and shallow asthenospheric upwelling beneath the rift axis would produce a large amount of melt, which is not observed as either underplate or surface volcanism. As we will show later, the patches of volcanic outcrops observed off-axis are well explained by a moderate heating of a deep-seated (70 km) asthenosphere.

Thermal and mechanical models

In this study, the Moho depth is used to define the crust/mantle rheological interface in the computation of the rheological yield stress envelopes, and the LAB is assumed to correspond to the 1330°C isotherm. We define a geographical grid comprised between 50°N and 58°N and 100°E and 117°E, which is converted into Cartesian coordinates with a spacing between grid points of 20 km. We use a 3D thermal model, which accounts for radiogenic heat production in the continental crust:

$$\frac{\delta T}{\delta t} = \kappa \Delta T + \frac{A}{\rho C_P} \qquad (1)$$

where T is the temperature, κ is the thermal diffusivity, A is the radiogenic heat production, ρ the density and C_P the specific heat (see Table 1 for constants description). Surface heat flow q_0 is computed from Fourier law: $q_0 = -k\nabla T_{(z=0)}$ and is compared with the values published in the compilation made by Pollack [1993]. We use as initial condition a steady state

continental geotherm with a flat lithosphere/asthenosphere boundary (defined as the depth to the 1330°C isotherm) at the base of the model (140 km). The topography of the 1330°C isotherm is then uplifted to the present-day position defined by the gravity models, and kept fixed for the rest of the experiment (cooling-plate model). The model runs during 20 Myrs, which is an approximation of the mean rifting duration. The predicted temperatures are compared to the peridotite solidus in order to determine whether partial melting of the mantle is possible or not.

Then, computed geotherms are then used to determine 2D yield stress envelopes (YSE) for every point of the grid using a brittle-elastic-ductile rheology for the crust and mantle layers [e.g., Burov and Diament, 1995]. Brittle failure is described by Byerlee's law [Byerlee, 1978]:

$$\sigma_3 = \sigma_b / 3.9 \text{ if } \sigma_3 < 120\,\text{MPa} \text{ and } \sigma_3 = \sigma_b / 2.1 - 100 \text{ if } \sigma_3 \geq 120\,\text{MPa}$$

Where σ_b (expressed in MPa) is the differential yield stress for brittle failure, $\sigma_b = \sigma_1 - \sigma_3$.

Ductile behavior is controlled by non-linear, temperature dependent dislocation creep:

$\sigma_d = \left(\dot{\varepsilon} A^{-1}\right)^{1/n} \exp\left(\frac{H}{nRT}\right)$ (see Table 1 for parameters names and values).

where σ_d is the differential stress for ductile flow, $\dot{\varepsilon}$ is the strain rate, R is the universal gas constant, and the parameters A, H and n are material-dependent. We primarily chose the commonly inferred values typical of mafic (diabase) compositions for the crust and of ultramafic (olivine) compositions for the mantle (Table 1). Although the uppermost crust may be quartz-rich, the choice of stronger ductile crustal rheology (corresponding to a deeper brittle-ductile transition) is dictated by the fact that previous studies have evidenced for a seismogenic crust down to at least 30 km in the Baikal rift [Déverchère et al., 1991; 2001]. Such deep seismic depth cannot be obtained with a more acid (i.e. quartz-dominated or feldspar-dominated) crustal composition. The chosen mean strain rate corresponds to an opening velocity of ~3mm/yr [Calais et al., 2003] over a 50 to 100 km-wide rift zone.

The yield stress envelopes (YSE) are defined as the contour of the maximal yield stress (either σ_d or σ_b) as function of depth. There are different sets of rock mechanics data that might produce quite different YSE for the same mineral composition, thermal and strain rate profile [Burov and Watts, 2006]. To validate the choice of the data provided in Table 1 for construction of "local" YSE for the Baikal area, we use the approach suggested in Burov and Diament [1992, 1995]. This technique allows one to constrain the YSE *in situ* using the EET estimates obtained from robust forward flexural models along selected profiles. As

shown in the referenced studies, one can constrain the shape of the local YSE provided that (1) EET, (2) thermal profile, (3) crustal thickness and (4) regional strain rate are known. These data are available from the previous studies [Burov et al., 1994; Petit et al., 1997, 2006]. At first stage, these parameters are used to compute the thickness of mantle and crustal (h_m and h_c, respectively) elastic "cores" and the position of the depths of brittle-ductile transition (BDT). The crust and mantle are mechanically decoupled if the brittle-ductile transition is located 10-15 km above the Moho, because in this case the strength of the lower crust is lower that tectonically sensible threshold of 10MPa.

The "decoupled" EET is computed from the equation [Burov and Diament, 1995]:

$$EET \approx \sqrt[3]{h_c^3 + h_m^3}$$

This equation follows from the general relation between the flexural rigidity of a stratified plate (compose of n decoupled layers) and its equivalent elastic thickness, EET:

$$D = \sum_{i=1}^{n} D_i(x) = \frac{E \cdot \sum_{i=1}^{n} h_i^3}{12(1-\nu^2)} = \frac{E \cdot EET^3}{12(1-\nu^2)}$$

where D is the flexural rigidity of the plate, E is Young modulus, ν is Poisson's ratio, and D_i and h_i refer to the flexural rigidities and thicknesses of i-th layer, respectively.

If the predicted crustal BDT depth is near the Moho, the crust and mantle are mechanically coupled, and the effective elastic thickness is up to twice higher than in the previous case: $EET = h_c + h_m$.

Results

The predicted surface heat flow in the Baikal rift exhibits low (50 mW/m^2) values in the Siberian craton and higher values (up to 65 mW/m^2) in the areas of thinner lithosphere, in the eastern and southwestern part of the rift. These results are consistent with the long-wavelength variations of the measured surface heat flow (Fig. 3), although the latter shows localised peak values of more than 90mW/m^2, which are not reproduced by the conductive model. These local highs are likely to correspond to hydrothermal circulation along major faults [Poort and Klerkx, 2004], rather than to conductive heat transfer. In the southwestern part of the rift, the observed local high of ~150 mW/m^2 corresponds to that of 65 mW/m^2 in the model and it is also shifted laterally towards the east (Fig. 3). This is probably due to a poor resolution of the LAB and Moho models at the grid boundaries. As a whole, we can consider that the conductive model provides a satisfactory smoothed estimate for the background surface heat flow of the Baikal rift. A better fit could be obtained by allowing the

conductivity to vary laterally and/or vertically, but we do not have any constraints on these possible variations.

The map of the predicted EET values suggests large lateral variations in the mechanical strength of the lithosphere: most of the Sayan-Baikal fold belt displays values lower than 35 km (due to the predicted crust-mantle decoupling) whereas the Siberian craton is characterized by EET values larger than 50 km (Fig. 4, crust-mantle coupling). The lack of intermediate values is due to the sharp change from coupled to decoupled behaviour causing a dramatic decrease of EET [up to 50%, see Burov and Diament, 1995]. The boundary between coupled and decoupled region closely follows the southern limit of the Siberian craton (Fig. 1). In the whole study area, the effective elastic thickness is never less than 20-30 km. The comparison between the predicted *EET* variations and the spatial distribution of earthquakes evidences for close relationships between the coupled/decoupled behaviour and strain localisation. In the central part of the rift zone (i.e. between 104°E and 110°E), the rift cuts through a mechanically coupled lithosphere and earthquake epicentres gather along a thin linear belt, suggesting that extensional deformation is localised along large-offset border faults in the crust, probably because of the large lithospheric strength. On the other hand, NE and SW of this zone, earthquake epicentres are spread over much wider areas which are entirely located within the predicted zone of decoupled lithosphere. It is worth noting that the deformation zone narrows again at the extreme NE of the rift system, when encountering another region of coupled lithosphere. A cross-section of the computed lithospheric strength across the rift depicts important variations of the elastic thickness of the mantle layer: whereas the base of the mechanical lithosphere (i.e., the depth below which the lithospheric strength becomes tectonically negligible) is as large as ~100 km beneath the Siberian craton, it decreases dramatically to ~60 km east of the rift. The present-day crustal deformation imaged by earthquakes, faults and lower crustal thinning is not located precisely above the area of thin mantle lithosphere but is offset ~200 km northwest of it (Fig 5).

Finally, with temperature of 1330°C at present LAB, the computed geotherms do not reach the peridodite solidus and partial melting does not occur (Fig. 6). This is consistent with the present-day situation where all volcanic centres are inactive. Mantle xenolith temperatures have evidenced a recent (~2 Ma) heating of the base of the lithosphere near the Vitim volcanic field [Ionov, 2002]. We tested another thermal model in which the last 2 Ma are characterized by a hotter asthenosphere temperature (1450°C). In this case, relatively thin melt zones (4 to 8 km-thick) would appear at the bottom of the lithosphere near the Hamar-Daban and Vitim volcanic fields (Fig. 6). The source of such moderate heating of the

asthenosphere is still unknown, but this phenomenon could explain the scattered magmatic activity encountered in the Baikal rift for at least 40 Ma.

Discussions and Conclusions

Most previous studies have quite consistently suggested high *EET* values of 30-50 km for the Baikal rift, and the Siberian craton lithosphere being stronger (EET ~ 60 km) than the Sayan-Baikal fold belt (EET ~30 km) [Burov et al., 1994; Petit et al., 1997; Ruppel et al., 1993; Van der Beek, 1997; Petit and Déverchère, 2006]. In contrast, spectral analysis (inversion) of the free-air gravity anomaly by Emmerson et al. [2006] yields much lower estimates (5-20 km) but still, the highest EET values are found over the craton. However, inverse gravity models can handle only continuous plates and often yield biased solutions, depending on which kind of gravity anomaly, FAA or Bouguer, is used [see discussion in Watts and Burov, 2003; Burov and Watts, 2006]. Fortunately, except the analysis of Emmerson et al. [2006] and the study of Diament and Kogan [1990] and Ruppel et al. [1993], the other EET estimates for Baikal rift zone are based on robust forward 2D flexural models that are, by definition, invariant to the type of the gravity data used and can handle discontinuous plates. These models demonstrate that the lithosphere does not behave as a single continuous plate, but that the Baikal rift presents a major mechanical and rheological discontinuity between two different plates, where plate flexure localises. Our results are in good agreement with most of these studies, and provide a map of predicted *EET* variations over the entire rift system. In the Siberian craton, the relatively thin crust and cold lithosphere favour a mechanical coupling between the crust and mantle, which explains a higher *EET*. The limit between the coupled and decoupled lithosphere closely fits the geometry of cratonic suture given by the surface geology, except beneath the central part of the rift where coupled lithosphere seems to extend SE of the suture, beneath the present-day deforming zone (Fig. 5).

The good correspondence between EET values predicted by flexural models and those computed from LAB and Moho depths allows us to conclude that (1) the laboratory based rock rheology data are good approximation to long-term rheology, and (2) that the mantle lithosphere contributes to the high lithospheric strength encountered in the Siberian craton but also in some parts of the Sayan-Baikal fold belt. In addition, gravity inversion combined with a simple thermal modelling and rheological laws classically used in thermo-mechanical models provide an estimate of the lithosphere rheology that explains the observed earthquake spatial distribution. It is very unlikely that such a good correlation can be found with a strong

crust alone, as the mechanical threshold from coupled to uncoupled behaviours would not exist.

Finally, the thermal model suggests that a moderate heating (120°C) of the base of the lithosphere could explain the occurrence of volcanism in the Vitim and Hamar-Daban area. This is in agreement with the xenolith analysis published by Ionov [2002], which showed that a temperature elevation of ~100°C is responsible for Pleistocene volcanism in the Vitim region. According to Barry et al. [2003], partial melting responsible for the Neogene basalts encountered in China, Mongolia and Baikal regions can be explained by a low heat flux thermal anomaly at the base of the lithosphere. The presence of such small anomaly is confirmed by recent seismic tomography data [Lebedev et al., 2006].

In conclusion, we show that EET values obtained from gravity models of the Moho and LAB interfaces combined with a simple conductive thermal model are very consistent with totally independent data (earthquake spatial distribution, surface geology) and demonstrate that the degree of crust-mantle coupling exerts a first-order control on the distribution of active deformation in the Baikal rift. Whether this situation has prevailed since the beginning of rifting is difficult to assess, as we can only image the present-day situation. The seismic belts are generally closely following active faults and rift basins, some of them being very old (around 30 Ma) in the central and southern parts of the rift. In any case, all these basins are not younger than 3-4 Ma [Petit and Déverchère, 2006 and references therein]. It is thus probable that the present-day situation has existed since at least the Mio-Pliocene "fast rifting" stage. Besides this, moderate heating of the asthenosphere in areas of thinner lithosphere can explain the localisation of volcanic fields, but this phenomenon is not clearly correlated with the localisation of tectonic deformation.

Acknowledgements. The authors are grateful to Cynthia Ebinger, Jeffrey Poort and an anonymous reviewer for their constructive reviews and to Claude Jaupart (editor) for his advices.

References

Barry, T. L., Saunders, A. D., Kempton, P. D., Windley, B. F., Pringle, M. S., Dorjnamjaa D., and Saandar, S., 2003. Petrogenesis of Cenozoic basalts from Mongolia: Evidence for the role of asthenospheric versus metasomatised mantle sources, *J. Petrol., 44*, 55-91.

Buck, W. R., 1991. Modes of continental lithospheric extension*, J. Geophys. Res., 96*, 20161-20178.

Burov, E. B., and Diament, M., 1995. The effective elastic thickness (Te) of continental lithosphere: What does it really mean ? *J. Geophys. Res., 100*, 3905-3927.

Burov, E.B. and Diament, M., 1992. Flexure of the continental lithosphere with multilayered rheology, Geophys. J. Int. 109, 449-468.

Burov, E.B., and Diament, M., 1996. Isostasy, equivalent thickness, and inelastic rheology of continents and oceans, *Geology*, *24*, 419-422.

Burov, E.B., Houdry, F., Diament, M., and Déverchère, J., 1994. A broken plate beneath the North Baikal rift zone revealed by gravity modelling, *Geophys. Res. Lett., 21*, 129-132.

Burov, E., and Poliakov, A., 2001. Erosion and rheology controls on syn- and post-rift evolution: verifying old and new ideas using a fully coupled numerical model, *J. Geophys. Res*., *106*, 16461-16481.

Burov, E. B. and Watts, A. B., 2006. "The long-term strength of continental lithosphere: "jelly sandwich" or "crème-brûlée"?", GSA Today, 16, 4-10.

Byerlee, J. D., 1978. Friction of rocks, *Pure Appl. Geophys.* 116, 615-626.

Calais, E., Vergnolle, M., Sankov, V., Lukhnev, A., Miroshnitchenko, A., Amarjargal, S., and Déverchere, J., 2003. GPS measurements of crustal deformation in the Baikal-Mongolia area (1994-2002): Implications for current kinematics of Asia, *J. Geophys. Res., 108*, doi:10.1029/2002JB002373.

Déverchère, J., Houdry, F., Diament, M., Solonenko, N. V., and Solonenko, A. V. 1991. Evidence for a seismogenic upper mantle and lower crust in the Baikal rift, *Geophys. Res. Lett., 18*, 1099-1102.

Déverchère, J., Petit, C., Gileva, N., Radziminovitch, N., Melnikova, V., and San'kov, V., 2001. Depth distribution of earthquakes in the Baikal Rift System and its implications for the rheology of the lithosphere, *Geophys. J. Int., 146*, 713-730.

De la Torre T. L., G. Monsalve, A. F. Sheehan, S. Sapkota and F. Wu, Earthquake processes of the Himalayan collision zone in eastern Nepal and the southern Tibetan Plateau, Geophys. J. Int., doi: 10.1111/j.1365-246X.2007.03537.x, 2007.

Diament, M., and M. Kogan, 1990. Long-wavelength gravity anomalies over the Baikal rift and geodynamic implications, *Geophys. Res. Lett.,* 17, 1977-1980.

Emmerson, B., Jackson, J., McKenzie, D., and Priestley, K., 2006. Seismicity, structure and rheology of the lithosphere in the Lake Baikal region, Geophys. J. Int., 167, 1233-1272.

Flesch L. M., Holt, W.E., Silver, P. G., Stephenson, M., Wang, C-Y., and Chan, W.W., 2005. Constraining the extent of crust–mantle coupling in central Asia using GPS, geologic, and shear wave splitting data, Earth Planet Sci. Lett., 238, 248– 268.

Gao, S., Liu, K. H., Davis, P. M., Slack, P. D., Zorin, Yu. A., Mordvinova, V. V. and Kozhevnikov, V. M., 2003. Evidence for small-scale mantle convection in the upper mantle beneath the Baikal rift zone, J. Geophys. Res., 108, doi:10.1029/2002JB002039.

Gao, S., Liu, K. H., and Chen, C., 2004. Significant crustal thinning beneath the Baikal rift zone: New constraints from receiver function analysis, *Geophys. Res. Lett., 31*, L20610, doi: 10.1029/2004GL020813.

Hopper, J. R., and Buck, R. W., 1998, Styles of extensional decoupling, Geology, 26, 699-702.

Huismans, R. S. and Beaumont, C., 2002. Asymmetric lithospheric extension:The role of frictional plastic strain softening inferred from numerical experiments, Geology, 30, 211-214.

Huismans, R.S., Podladchikov, Yu. Y., and Cloetingh, S., 2001. Transition from passive to active rifting: relative importance of asthenospheric doming and passive extension of the lithosphere, J. Geophys. Res. 106, 11,271-11,291.

Ionov, D., 2002. Mantle structure and rifting processes in the Baikal-Mongolia region: geophysical data and evidence from xenoliths in volcanic rocks, *Tectonophysics, 351*, 41-60.

Lavier, L.L. and Manatschal, G., 2006, A mechanism to thin the continental lithosphere at magma-poor margins, Nature, 440, 324-328.

Lebedev, S., Mier, T., and van der Hilst, R.D., 2006. Asthenospheric flow and origin of volcanism in the Baikal Rift area, *Earth and Planet. Sci. Lett.*, *249*, 415-424.

Logatchev, N. A., and Florensov, N. A., 1978. the Baikal system of rift valleys, *Tectonophysics, 45*, 1-13.

Maggi, A., J.A. Jackson, D. McKenzie, and K. Priestley, 2000. Earthquake focal depths, effective elastic thickness, and the strength of the continental lithosphere, *Geology*, *28*, 495-498.

Monsalve G., A. Sheehan, V. Schulte-Pelkum, S. Rajaure, M. R. Pandey, and F. Wu, Seismicity and one-dimensional velocity structure of the Himalayan collision zone: Earthquakes in the crust and upper mantle, *J. Geophys. Res*., 111, B10301, doi:10.1029/2005JB004062, 2006

Mouthereau, F. and Petit, C., 2003. Rheology and strength of the Eurasian continental lithosphere in the foreland of the Taiwan collision belt: Constraints from seismicity, flexure, and structural styles, J. Geophys. Res., 108, doi: 10.1029/2002JB002098.

Park, S. K., Jiracek, G. R., and Johnson, K. M., 1992. Magnetotelluric evidence for a brittle-ductile transition, Peninsular Ranges Batholith, Southern California? Geophys. Res. Letters 19, 2143-2146.

Pavlenkova, G. A., Priestley, K., and Cipar, J., 2002. 2D model of the crust and uppermost mantle along rift profile, Siberian craton, *Tectonophysics, 355*, 171-186.

Petit, C., Burov, E. B., and Déverchère, J., 1997. On the structure and mechanical behavior of the extending lithosphere in the Baikal rift from gravity modelling, *Earth Planet. Sci. Lett., 149*, 29-42.

Petit, C. and Déverchère, J., 2006. Structure and evolution of the Baikal rift: a synthesis, Geochem. Geophys. Geosyst., 7, doi:10.1029/2006GC001265.

Pollack, H.N., Hurter, S.J., and Johnson, J.R., 1993. Heat flow from the earth's interior: analysis of the global data set, *Reviews of Geophysics, 31*, 267-280.

Poort, J., and Klerkx, J., 2004. Absence of a regional surface thermal high in the Baikal rift; new insights from detailed contouring of heat flow anomalies, *Tectonophysics, 383*, 217-241.

Rasskazov S. V., Luhr J. F., Bowring S. A., Ivanov A. V., Brandt I. S., Brandt S. B., Demonterova E. I., Boven A. A., Kunk M., Housh T., Dungan M. A., 2002. Late Cenozoic Volcanism in the Baikal Rift System: Evidence for Formation of the Baikal and Khubsugul Basins due to Thermal Impacts on the Lithosphere and Collision-Derived Tectonic Stress, *International Symposium - Speciation in Ancient Lakes, SIAL III - Irkutsk, September 2-7, 33-48.*

Ruppel, C., Kogan, M. G., and McNutt, M. K., 1993. Implications of new gravity data for the Baikal rift zone structure, *Geophys. Res. Lett., 20*, 1635-1638.

Stich, D., Mancilla, F.L., and Morales, J., 2005. Crust-mantle coupling in the Gulf of Cadiz (SW-Iberia), Geophys. Res. Lett., 32, doi:10.1029/2005GL023098.

Suvorov, V. D., Mishenkina, Z. M., Petrick, G. V., Sheludko, I. F., Seleznev, V. S., and Solovyov, V. M., 2002. Structure of the crust in the Baikal Rift Zone and adjacent areas from Deep Seismic Sounding data, *Tectonophysics, 351*, 61-74.

Tibéri C., Diament, M., Déverchère, J., Petit, C., Mikhailov, V., Tikhotsky, S., and Achauer, U., 2003. Deep structure of the Baikal rift zone revealed by joint inversion of gravity and seismology, *J. Geophys. Res., 108*, doi : 10.1029/2002JB001880.

Van der Beek, P., Delvaux, D., Andriessen, P. A. M., and Levi, K. G., 1999. Early cretaceous denudation related to convergent tectonics in the Baikal region, SE Siberia, *J. Geol. Soc. London, 153*, 515-523.

Watts, A. B. and Burov, E. B., 2003. "Lithospheric strength and its relationship to the elastic and seismogenic layer thickness", Earth Planet. Sci. Letts., 213, 113-131.

Figure captions

Fig 1. Earthquake epicenters, active faults, basins and volcanic centres in the Baikal rift [after Petit and Déverchère, 2006]. Inset shows the location of the Baikal rift in Asia. Thick grey dashed line delineates the southern boundary of the Siberian craton.

Fig 2. Depths to the Moho (top panel) and lithosphere-asthenosphere boundary (bottom panel) deduced from gravity data [after Petit and Déverchère, 2006]. Dark grey dots are earthquake epicentres.

Fig 3. Top: measured surface heat flow in mW/m^2 [after Pollack, 1993]. Bottom: modelled surface heat flow (this study). Dark grey dots are earthquake epicentres.

Fig 4. Effective elastic thickness of the lithosphere as predicted from thermo-rheological model [in km]. Dark grey dots are earthquake epicentres.

Fig 5. Lithospheric strength profile (see location on Fig. 4). The position of the brittle/ductile transition in the crust and of the base of mechanical lithosphere (defined as the depth of peak resistance in the crust and of negligible resistance in the mantle, respectively) are indicated. Stars symbolize earthquakes foci beneath the rift down to depths of ~30 km [Déverchère et al., 2001]. Inset shows two schematic yield-stress envelopes for a coupled (A) and uncoupled lithosphere (B). Open rectangles A and B show their corresponding position on the strength profile.

Fig 6. Predicted thickness of the melt zone at the bottom of the lithosphere in km for temperatures at the LAB of 1330°C (top) and 1450°C (bottom).

FIGURE 1

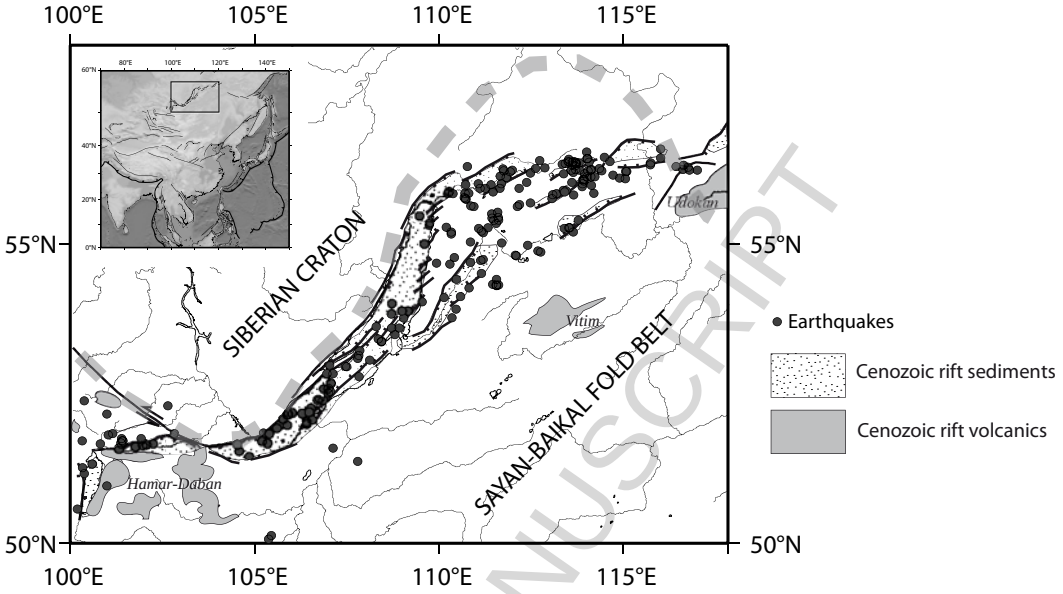

FIGURE 2

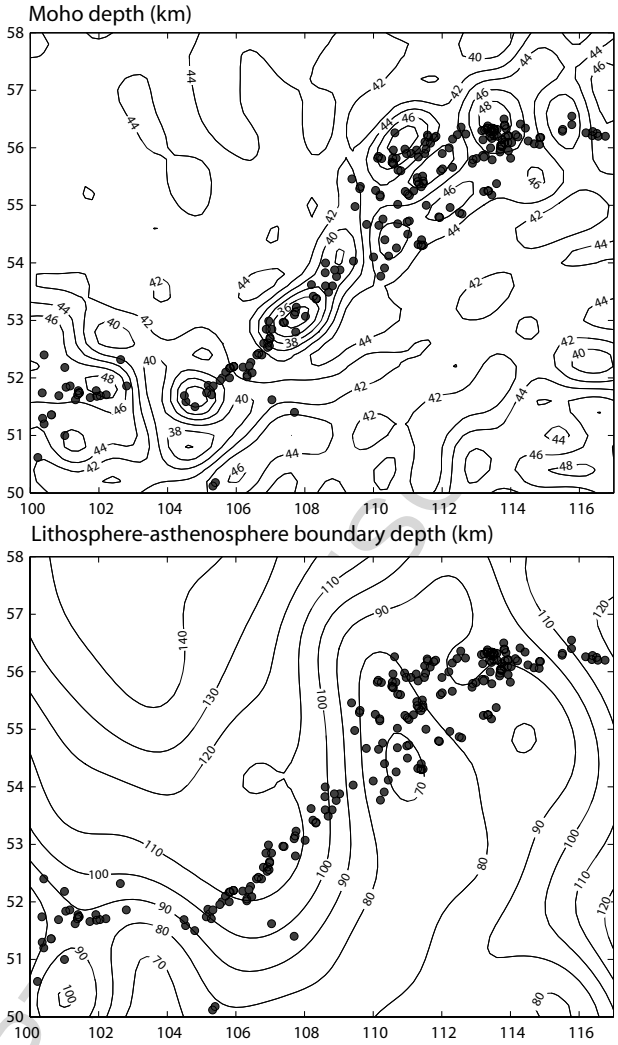

FIGURE 3

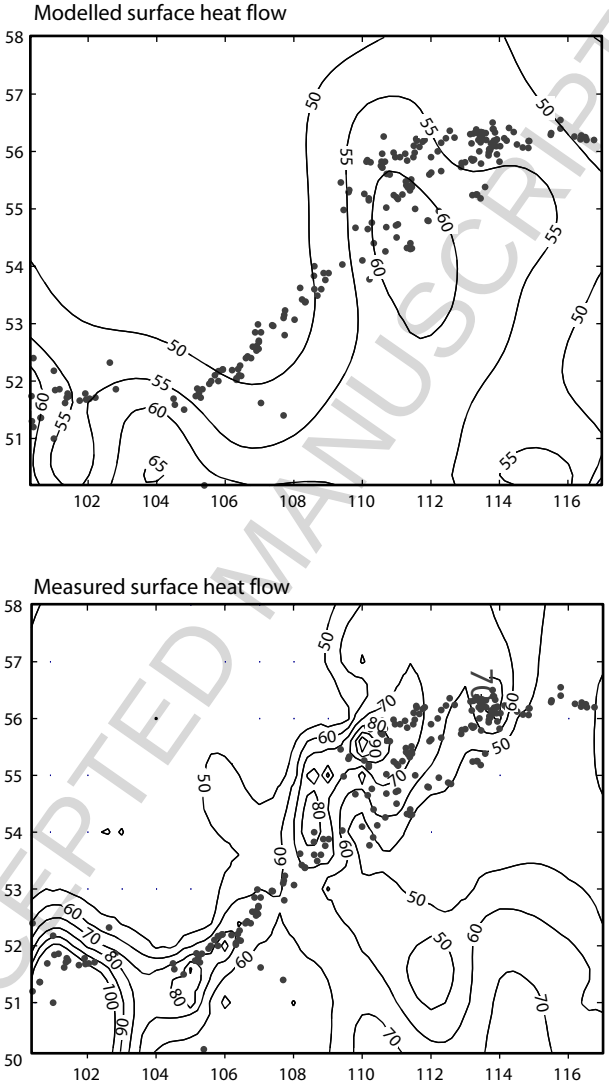

FIGURE 4

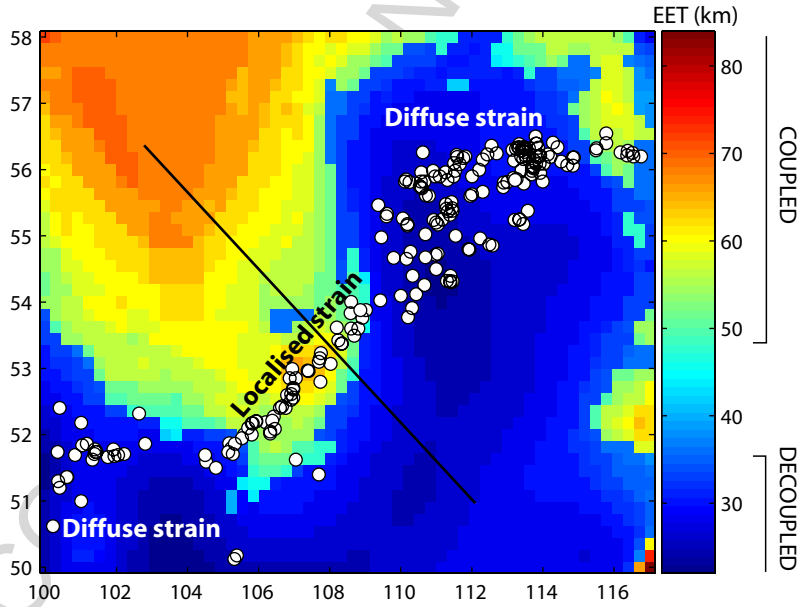

Figure 5

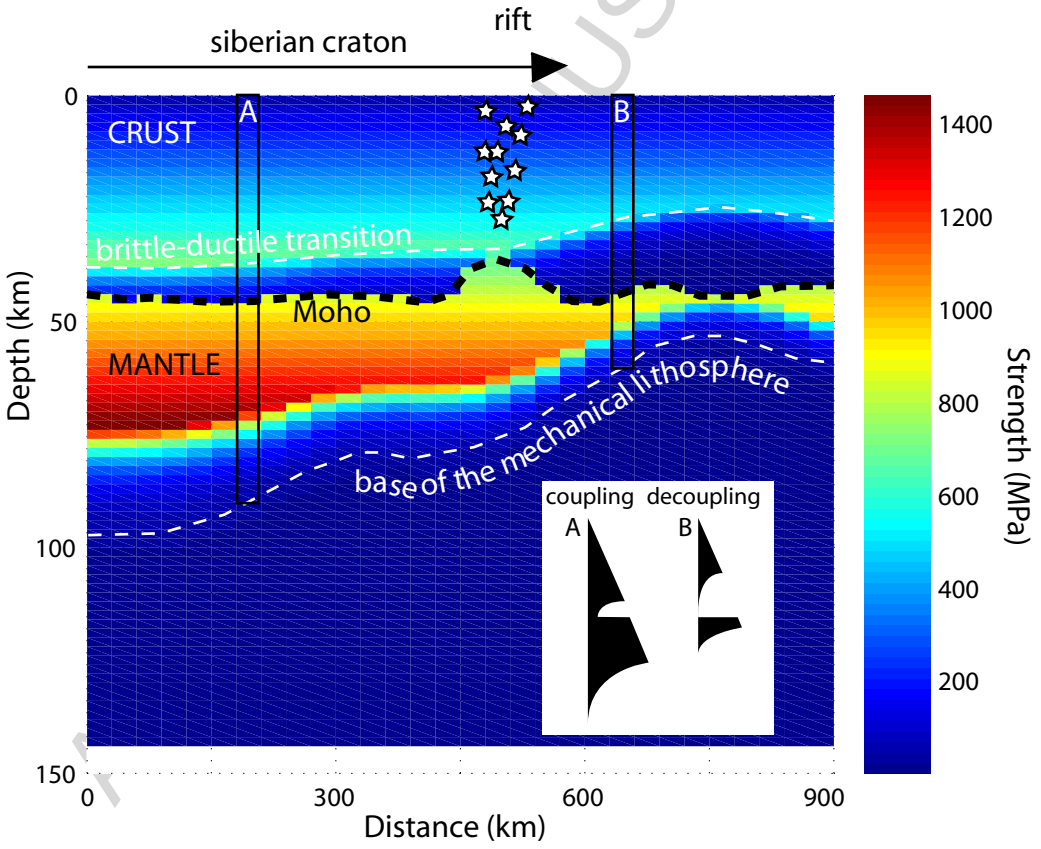

FIGURE 6

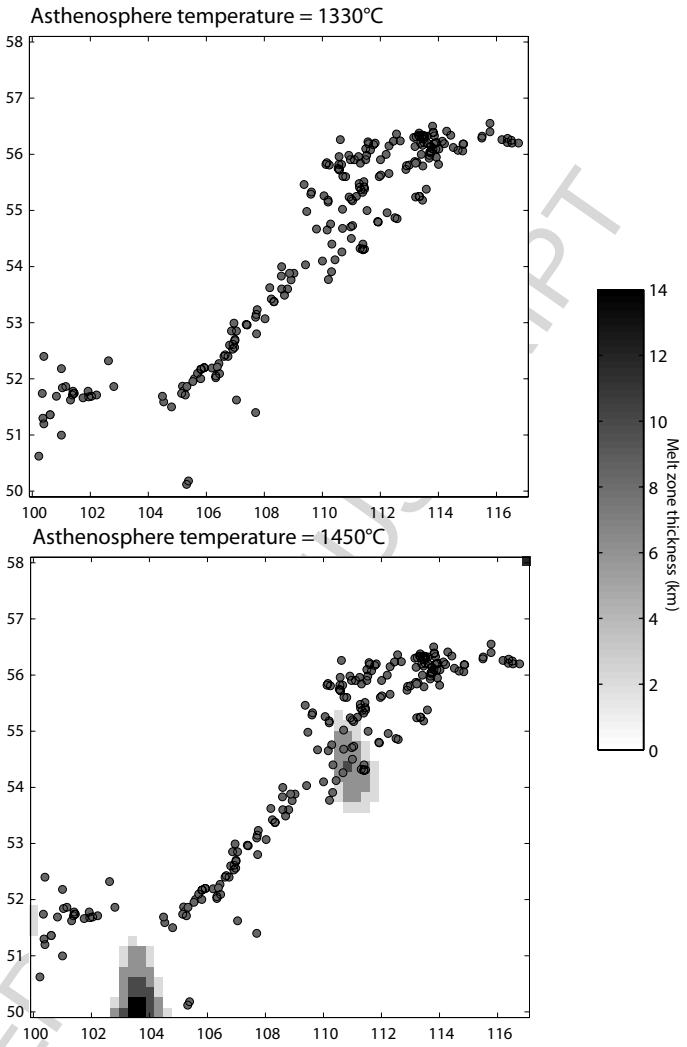

Table 1. Parameter values and description

Symbol	Description	Value
κ	Thermal diffusivity	$1e^{-6}$ m^2. s^{-1}
ρ_c	Crust density	2700 $kg.m^{-3}$
ρ_m	Mantle density	3200 $kg.m^{-3}$
H_0	Surface radiogenic heat production	$3.10^{-6} W.kg^{-1}$
Z_r	radiogenic decay length scale	10 km
$\dot{\varepsilon}$	Strain rate	$10^{-15} s^{-1}$
A	Flow law material constant	6.31 $10^{-20} Pa^{-n} s^{-1}$ (crust)
		7.00 $10^{-14} Pa^{-n} s^{-1}$ (mantle)
n	Flow law strain exponent	3.05 (crust)
		3.00 (mantle)
H	Flow law activation enthalpy	276 kJ mol^{-1} (crust)
		520 kJ mol^{-1} (mantle)
R	Gas constant	8.301 J mol^{-1} K^{-1}